

Supporting Information for

**Rational prediction of multifunctional bilayer single atom catalysts for hydrogen evolution, oxygen evolution and oxygen reduction reaction**

Riming Hu<sup>a</sup>, Yongcheng Li<sup>a</sup>, Fuhe Wang<sup>b</sup>, Jiaxiang Shang<sup>a,\*1</sup>

<sup>a</sup>School of Materials Science and Engineering, Beihang University, Beijing, 100191, China

<sup>b</sup>Center for condensed matter physics, Department of Physics, Capital Normal University, Beijing 100048, China

---

\* Corresponding author. E-mail: shangjx@buaa.edu.cn (Jia-Xiang Shang)

**Calculation details of adsorption energy (E), zero-point energy (ZPE), entropy (S), and the free energy correction of the pH ( $\Delta G_{pH}$ ).**

The adsorption energies of all reaction intermediates are calculated as:

$$\Delta E_{O^*} = E(O^*) - E(*) - [E(H_2O) - E(H_2)] \quad (S1)$$

$$\Delta E_{OH^*} = E(OH^*) - E(*) - [E(H_2O) - 1/2E(H_2)] \quad (S2)$$

$$\Delta E_{OOH^*} = E(OOH^*) - E(*) - [2E(H_2O) - 3/2E(H_2)] \quad (S3)$$

$$\Delta E_{H^*} = E(H^*) - E(*) - 1/2E(H_2) \quad (S4)$$

where  $E(*)$ ,  $E(O^*)$ ,  $E(OH^*)$ ,  $E(OOH^*)$  and  $E(H^*)$  are the DFT total energies of a clean catalyst surface, and that adsorbed by a  $O^*$ ,  $OH^*$ ,  $OOH^*$  and  $H^*$  species, respectively;  $E(H_2O)$  and  $E(H_2)$  are the energies of a  $H_2O$  and  $H_2$  molecule in vacuum, respectively.

ZPE is defined as:

$$ZPE = \sum_i \frac{1}{2} h\nu_i \quad (S5)$$

where  $i$  is the frequency number,  $\nu_i$  is the frequency with unit  $\text{cm}^{-1}$ .

The entropies of  $H_2O$ ,  $O_2$ , and  $H_2$  are obtained from the NIST database with standard condition, and the adsorbed species were only taken vibrational entropy (S) into account, as shown in the following formula:

$$S = \sum_i R \left\{ \frac{h\nu_i}{k_B T} \left[ \exp\left(\frac{h\nu_i}{k_B T}\right) - 1 \right]^{-1} - \ln \left[ 1 - \exp\left(-\frac{h\nu_i}{k_B T}\right) \right] \right\} \quad (S6)$$

where  $R = 8.314 \text{ J}\cdot\text{mol}^{-1}\cdot\text{K}^{-1}$ ,  $T = 298.15 \text{ K}$ ,  $h = 6.63 \times 10^{-34} \text{ J}\cdot\text{s}$ ,  $k_B = 1.38 \times 10^{-23} \text{ J}\cdot\text{K}^{-1}$ ,  $i$  is the frequency number,  $\nu_i$  is the vibrational frequency (unit is  $\text{cm}^{-1}$ ).

$\Delta G_{pH}$  is the correction of the  $H^+$  free energy and depends on whether the reaction under consideration is a reduction or an oxidation.

$$\Delta G_{pH} = -k_B T \ln[H^+] = \text{pH} \times k_B T \ln 10 \quad (S7)$$

Hence, the equilibrium potential for four-electron transfer ORR at  $\text{pH} = 0$  ( $\text{pH} = 14$ ) was determined to be 1.23 V (0.40 V).

## The ORR and OER process in alkaline environment

The ORR process in alkaline environment can be described as:

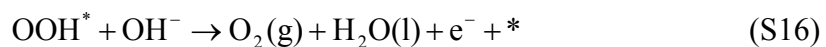
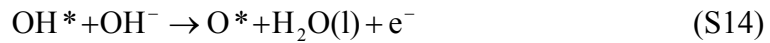


The ORR may proceed through the following elementary steps, which are usually employed to investigate the electrocatalysis of the ORR on various materials:



where  $*$  stands for an active site on the catalytic surface, (l) and (g) refer to liquid and gas phases, respectively.

The OER occurring in an alkaline electrolyte through elementary steps takes the reverse direction of ORR:



### **Calculation details of formation energy ( $E_f$ ) for monolayer MN<sub>4</sub>**

The  $E_f$  of monolayer MN<sub>4</sub> is defined as

$$E_f = E_{MN_4} - E_{N_4} - E_M \quad (S17)$$

in which  $E_{MN_4}$  and  $E_{N_4}$  indicate the energy of monolayer MN<sub>4</sub> and N-coordination graphene, respectively.  $E_M$  is the energies of the transition metal atom in the bulk crystal.

## Supercell $5 \times 3$ vs $3 \times 2$

To investigate the effect of model size on catalytic performance, we build the period  $3 \times 2$  and  $5 \times 3$  rectangular graphene supercell, respectively. Calculated adsorption free energies ( $\Delta G_{O^*}$ ,  $\Delta G_{OH^*}$ , and  $\Delta G_{OOH^*}$ ) and overpotentials ( $\eta^{ORR}$  and  $\eta^{OER}$ ) on  $FeN_4$  and  $Fe/Hf$  with different sizes are listed in Table S1. One can see that the values of adsorption free energies and overpotentials for  $3 \times 2$  and  $5 \times 3$  models are very close (not more than 0.1 eV/V), which indicates that the period  $3 \times 2$  rectangular graphene supercell is large enough to avoid the interaction between two neighboring metal atoms.

**Table S1.** Calculated adsorption free energies of reaction intermediates and overpotential for ORR and OER on  $FeN_4$  and  $Fe/Hf$  with  $3 \times 2$  and  $5 \times 3$  supercell.

supercell	FeN <sub>4</sub>					Fe/Hf				
	$\Delta G_{O^*}$ (eV)	$\Delta G_{OH^*}$ (eV)	$\Delta G_{OOH^*}$ (eV)	$\eta^{ORR}$ (V)	$\eta^{OER}$ (V)	$\Delta G_{O^*}$ (eV)	$\Delta G_{OH^*}$ (eV)	$\Delta G_{OOH^*}$ (eV)	$\eta^{ORR}$ (V)	$\eta^{OER}$ (V)
$3 \times 2$	1.68	0.74	3.54	0.49	0.63	2.25	0.85	3.75	0.38	0.27
$5 \times 3$	1.72	0.80	3.56	0.43	0.61	2.33	0.87	3.88	0.36	0.32

## PBE vs PBE + U

The multiple spin states are the essential role of the transition metal, which may vary the total energy of considered system. Therefore, it is crucial to ensure the accuracy of magnetic moment for the system containing transition metals. We also pay special attention to this issue. And the magnetic moments calculated (the GGA-PBE method is used in this work) in this paper are compared with those reported previously, it is found that they are consistent. For instance, the calculated magnetic moments are 3.00, 1.98, 0.81, and 0  $\mu_B$  for  $MnN_4$ ,  $FeN_4$ ,  $CoN_4$ , and  $NiN_4$ , which is consistent with previous reports (the reported magnetic moments for  $MnN_4$ ,  $FeN_4$ ,  $CoN_4$ , and  $NiN_4$  are -3.06, -1.97, 0.62, and 0  $\mu_B$  [1-3]).

In addition, to evaluate the accuracy of PBE results, we have calculated the magnetic moment of monolayer and bilayer SACs by PBE+U method. Note that the DFT+U approach also suffers from a strong (linear) dependence of the energetics on the choice of the value of the parameter U, and on the choice of the localized projector functions that enter the definition of the U-dependent energy term. According to previous reports [4], the U-J parameters for PBE+U calculations listed in Table S2 are employed.

**Table S2.** The values of U-J parameters for PBE+U calculations.

3d	Sc	Ti	V	Cr	Mn	Fe	Co	Ni	Cu	Zn
U-J	2.11	2.58	2.72	2.79	3.06	3.29	3.42	3.40	3.87	4.12

We first compared the magnetic moments of monolayer and bilayer SACs by employing PBE and PBE+U methods, the calculated results are listed in Table S3. It can be found that the magnetic moment of these systems are almost the same before and after using PBE+U method (not more than 0.1). The magnetic moments of the adsorption systems of reaction intermediates (including  $O^*$ ,  $OH^*$ , and  $OOH^*$ ) on  $FeN_4$  and  $Fe/Hf$  are also examined (Table S4). And the calculated magnetic moments by using PBE and PBE+U methods are also consistent. Thus, the method of GGA+PBE provides us an effective tool to accurately describe the magnetic moments of the models described in this paper.

**Table S3.** Calculated magnetic moment ( $\mu_B$ ) of monolayer and bilayer SACs before and after using PBE+U method.

Model	ScN <sub>4</sub>	TiN <sub>4</sub>	VN <sub>4</sub>	CrN <sub>4</sub>	MnN <sub>4</sub>	FeN <sub>4</sub>	CoN <sub>4</sub>	NiN <sub>4</sub>	CuN <sub>4</sub>	ZnN <sub>4</sub>
PBE	0.33	1.58	2.66	3.78	3.00	1.98	0.81	0	-1.00	0
PBE+U	0.33	1.48	2.74	3.88	3.00	1.98	0.81	0	-0.99	0
Model	Fe/Sc	Fe/Ti	Fe/V	Fe/Cr	Fe/Mn	Fe/Fe	Fe/Co	Fe/Ni	Fe/Cu	Fe/Zn
PBE	0	0	-0.78	4.00	-1.15	3.08	1.67	1.82	-1.06	1.16
PBE+U	0	0	-0.79	3.91	-1.24	2.99	1.73	1.81	-1.09	1.03

**Table S4.** Calculated magnetic moment ( $\mu_B$ ) of the adsorption system for reaction intermediates on monolayer and bilayer SACs before and after using PBE+U method.

Model	FeN <sub>4</sub>			Fe/Hf		
	intermediates	O	OH	OOH	O	OH
PBE	0	1.00	1.00	-1.57	0	-0.97
PBE+U	0	1.01	1.00	-1.61	0	-0.89

Furthermore, note that the results based on the GGA-PBE (the method used in this work) showed very good high performance in understanding the reaction mechanisms and activity trends observed in experiments [5, 6].

Due to the above reasons, we did not use PBE+U method to consider the effect of the highly localized orbitals of the metal atoms in this work.

## HER activity for BACs that adjacent bimetallic atoms both shown on the surface

The HER activity on BACs (take Fe-Cu as an example) that adjacent bimetallic atoms both shown on the surface is investigated. Calculated adsorption free energy for H\* ( $\Delta G_{H^*}$ ) is shown in Fig. S1. Note that the top site of Cu atom in monolayer Fe-Cu BACs is not a stable adsorption site for H atom, which will move to the bridge site between Fe and Cu atoms after geometry optimization. It can be found from Fig. S1 that the binding energy of H atom on monolayer Fe-Cu BACs is obviously stronger than that of on bilayer Fe/Cu. As a result, the formation from H\* to H<sub>2</sub> on monolayer Fe-Cu BACs is relatively difficult, which indicates a relatively low HER performance.

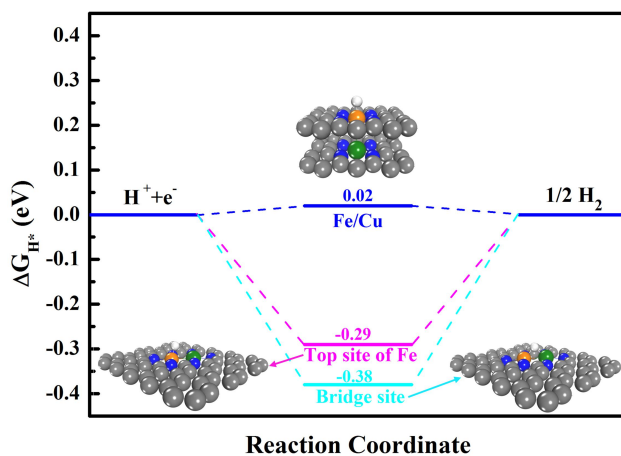


**Fig. S1.** The  $\Delta G_{H^*}$  for the monolayer BACs and B-SACs (Fe/Cu). The adsorption configuration of H atom is also shown in the figure, the white, gray, blue, orange, and green spheres indicate the H, C, N, Fe, and Cu atoms, respectively.

**Table S5.** Calculated ZPE and T×S of gas molecules and reaction intermediates adsorbed on catalysts, the ZPE values are averaged over all catalysts since they have rather close value.

Species	T×S (298K)	ZPE
	(eV)	(eV)
H*	0	0.15
O*	0	0.12
OH*	0	0.35
OOH*	0	0.43
H <sub>2</sub> (g)	0.41	0.27
H <sub>2</sub> O(g)	0.58	0.57

**Table S6.** The distance between two metal atoms ( $L_{Fe-M}$ ) and the interlayer distances (the difference between the average heights of two layers of atoms,  $d_{int}$ ) of B-SACs systems.

Model	$L_{Fe-M}$ (Å)	$d_{int}$ (Å)	Model	$L_{Fe-M}$ (Å)	$d_{int}$ (Å)	Model	$L_{Fe-M}$ (Å)	$d_{int}$ (Å)
Fe/Sc	2.51	3.44	Fe/Y	2.69	3.54	Fe/La	2.75	3.60
Fe/Ti	2.13	3.25	Fe/Zr	2.40	3.33	Fe/Hf	2.39	3.18
Fe/V	2.09	3.22	Fe/Nb	2.17	3.22	Fe/Ta	2.21	3.10
Fe/Cr	2.64	3.31	Fe/Mo	2.14	3.19	Fe/W	2.15	3.06
Fe/Mn	2.77	3.35	Fe/Tc	2.11	3.17	Fe/Re	2.14	3.07
Fe/Fe	2.79	3.33	Fe/Ru	2.30	3.18	Fe/Os	2.27	3.10
Fe/Co	2.76	3.30	Fe/Rh	2.64	3.24	Fe/Ir	2.59	3.21
Fe/Ni	3.16	3.43	Fe/Pd	3.19	3.45	Fe/Pt	3.06	3.37
Fe/Cu	3.04	3.39	Fe/Ag	2.52	3.51	Fe/Au	3.33	3.59
Fe/Zn	2.51	3.33	Fe/Cd	2.53	3.51	Fe/Hg	2.48	3.49

**Table S7.** Calculated formation energies ( $E_f$ ) of monolayer SACs.

	ScN <sub>4</sub>	TiN <sub>4</sub>	VN <sub>4</sub>	CrN <sub>4</sub>	MnN <sub>4</sub>	FeN <sub>4</sub>	CoN <sub>4</sub>	NiN <sub>4</sub>	CuN <sub>4</sub>	ZnN <sub>4</sub>
$E_f$ /eV	-4.30	-2.98	-2.28	-2.21	-2.40	-2.60	-2.41	-2.55	-1.35	-2.29
	YN <sub>4</sub>	ZrN <sub>4</sub>	NbN <sub>4</sub>	MoN <sub>4</sub>	TcN <sub>4</sub>	RuN <sub>4</sub>	RhN <sub>4</sub>	PdN <sub>4</sub>	AgN <sub>4</sub>	CdN <sub>4</sub>
$E_f$ /eV	-4.10	-2.51	-1.09	0.33	0.15	-0.01	-0.33	-1.55	-0.89	0.11
	LaN <sub>4</sub>	HfN <sub>4</sub>	TaN <sub>4</sub>	WN <sub>4</sub>	ReN <sub>4</sub>	OsN	IrN <sub>4</sub>	PtN <sub>4</sub>	AuN <sub>4</sub>	HgN <sub>4</sub>
$E_f$ /eV	-3.93	-2.46	-0.44	1.28	0.77	0.39	-0.12	-1.47	-0.02	0.22

**Table S8.** The adsorption free energy of H\* ( $\Delta G_{H^*}$ ), O\* ( $\Delta G_{O^*}$ ), OH\* ( $\Delta G_{OH^*}$ ), and OOH\* ( $\Delta G_{OOH^*}$ ) on Fe/M.

	$\Delta G_{H^*}$ (eV)	$\Delta G_{O^*}$ (eV)	$\Delta G_{OH^*}$ (eV)	$\Delta G_{OOH^*}$ (eV)
Fe/Sc	0.48	1.76	0.74	3.75
Fe/Ti	1.16	2.85	1.59	4.63
Fe/V	1.30	3.00	1.66	4.72
Fe/Cr	0.50	1.81	0.86	3.85
Fe/Mn	0.74	1.85	1.11	4.01
Fe/Fe	0.73	1.95	1.03	4.03
Fe/Co	0.59	1.93	1.01	4.00
Fe/Ni	0.41	1.56	0.69	3.67
Fe/Cu	0.02	1.18	0.33	3.30
Fe/Zn	0.67	1.92	1.05	4.02
Fe/Y	0.53	1.69	0.74	3.57
Fe/Zr	0.83	1.84	1.19	4.22
Fe/Nb	1.41	3.08	1.66	4.71
Fe/Mo	1.48	3.49	1.66	4.74
Fe/Tc	1.46	3.27	1.64	4.74
Fe/Ru	0.88	2.33	1.26	4.28
Fe/Rh	0.18	1.90	0.60	3.59
Fe/Pd	0.43	1.61	0.74	3.73
Fe/Ag	0.35	1.54	0.62	3.60
Fe/Cd	0.76	2.11	1.04	4.04
Fe/La	0.40	1.58	0.66	3.67
Fe/Hf	0.91	2.25	0.85	3.75
Fe/Ta	1.48	3.30	1.71	4.76
Fe/W	1.59	3.61	1.73	4.78
Fe/Re	1.52	3.55	1.65	4.74
Fe/Os	1.06	2.68	1.45	4.48
Fe/Ir	0.60	2.06	1.03	4.03
Fe/Pt	0.45	1.62	0.75	3.74
Fe/Au	-0.05	1.16	0.29	3.27
Fe/Hg	0.75	2.09	0.93	3.93
FeN <sub>4</sub>	-0.25	1.68	0.74	3.54

**Table S9.** The adsorption free energy of H\* ( $\Delta G_{H^*}$ ), O\* ( $\Delta G_{O^*}$ ), OH\* ( $\Delta G_{OH^*}$ ), and OOH\* ( $\Delta G_{OOH^*}$ ) on M/Fe.

	$\Delta G_{H^*}$ (eV)	$\Delta G_{O^*}$ (eV)	$\Delta G_{OH^*}$ (eV)	$\Delta G_{OOH^*}$ (eV)
Sc/Fe	2.03	4.14	-0.42	5.09
Ti/Fe	1.93	0.61	0.55	4.14
V/Fe	1.75	0.54	0.58	1.50
Cr/Fe	0.61	0.78	0.28	3.59
Mn/Fe	-0.04	0.77	0.15	2.04
Fe/Fe	0.73	1.95	1.03	4.03
Co/Fe	0.59	3.13	1.38	4.38
Ni/Fe	1.57	4.04	2.04	4.94
Cu/Fe	1.23	3.61	1.46	4.52
Zn/Fe	2.62	3.67	1.07	5.04
Y/Fe	2.49	5.04	2.57	5.05
Zr/Fe	2.17	0.85	2.08	5.15
Nb/Fe	1.99	0.42	1.88	4.99
Mo/Fe	1.78	0.30	1.83	4.90
Tc/Fe	1.58	1.23	1.79	4.97
Ru/Fe	0.51	1.99	1.08	4.18
Rh/Fe	0.31	2.93	0.92	3.99
Pd/Fe	1.95	4.55	2.27	5.04
Ag/Fe	-0.78	5.24	2.86	4.83
Cd/Fe	-0.19	5.11	2.84	4.94
La/Fe	0.31	4.99	2.75	4.87
Hf/Fe	2.05	0.49	1.83	4.96
Ta/Fe	1.82	0.36	1.63	4.73
W/Fe	1.67	0.26	1.63	4.74
Re/Fe	1.50	0.69	1.67	4.80
Os/Fe	0.76	1.81	1.25	4.41
Ir/Fe	0.25	3.03	1.27	4.39
Pt/Fe	1.45	4.20	2.01	4.93
Au/Fe	1.75	4.21	2.16	4.54
Hg/Fe	-0.77	5.11	2.84	4.84

**Table S10.** The free energy change of every reaction step for ORR ( $\Delta G_a$ - $\Delta G_d$ ) and OER ( $\Delta G_e$ - $\Delta G_h$ ) on Fe/M.

	ORR				OER			
	$\Delta G_a$ (eV)	$\Delta G_b$ (eV)	$\Delta G_c$ (eV)	$\Delta G_d$ (eV)	$\Delta G_e$ (eV)	$\Delta G_f$ (eV)	$\Delta G_g$ (eV)	$\Delta G_h$ (eV)
Fe/Sc	-1.17	-1.99	-1.02	-0.74	0.74	1.02	1.99	1.17
Fe/Ti	-0.29	-1.78	-1.26	-1.59	1.59	1.26	1.78	0.29
Fe/V	-0.20	-1.72	-1.34	-1.66	1.66	1.34	1.72	0.20
Fe/Cr	-1.07	-2.04	-0.95	-0.86	0.86	0.95	2.04	1.07
Fe/Mn	-0.91	-2.16	-0.74	-1.11	1.11	0.74	2.16	0.91
Fe/Fe	-0.89	-2.08	-0.92	-1.03	1.03	0.92	2.08	0.89
Fe/Co	-0.92	-2.07	-0.92	-1.01	1.01	0.92	2.07	0.92
Fe/Ni	-1.25	-2.11	-0.87	-0.69	0.69	0.87	2.11	1.25
Fe/Cu	-1.62	-2.12	-0.85	-0.33	0.33	0.85	2.12	1.62
Fe/Zn	-0.90	-2.10	-0.87	-1.05	1.05	0.87	2.10	0.90
Fe/Y	-1.35	-1.88	-0.95	-0.74	0.74	0.95	1.88	1.35
Fe/Zr	-0.70	-2.38	-0.65	-1.19	1.19	0.65	2.38	0.70
Fe/Nb	-0.21	-1.63	-1.42	-1.66	1.66	1.42	1.63	0.21
Fe/Mo	-0.18	-1.25	-1.83	-1.66	1.66	1.83	1.25	0.18
Fe/Tc	-0.18	-1.47	-1.63	-1.64	1.64	1.63	1.47	0.18
Fe/Ru	-0.64	-1.95	-1.07	-1.26	1.26	1.07	1.95	0.64
Fe/Rh	-1.33	-1.69	-1.30	-0.60	0.60	1.30	1.69	1.33
Fe/Pd	-1.19	-2.12	-0.87	-0.74	0.74	0.87	2.12	1.19
Fe/Ag	-1.32	-2.06	-0.92	-0.62	0.62	0.92	2.06	1.32
Fe/Cd	-0.88	-1.93	-1.07	-1.04	1.04	1.07	1.93	0.88
Fe/La	-1.25	-2.09	-0.92	-0.66	0.66	0.92	2.09	1.25
Fe/Hf	-1.17	-1.50	-1.40	-0.85	0.85	1.40	1.50	1.17
Fe/Ta	-0.16	-1.46	-1.59	-1.71	1.71	1.59	1.46	0.16
Fe/W	-0.14	-1.17	-1.88	-1.73	1.73	1.88	1.17	0.14
Fe/Re	-0.18	-1.19	-1.90	-1.65	1.65	1.90	1.19	0.18
Fe/Os	-0.44	-1.80	-1.23	-1.45	1.45	1.23	1.80	0.44
Fe/Ir	-0.89	-1.97	-1.03	-1.03	1.03	1.03	1.97	0.89
Fe/Pt	-1.18	-2.12	-0.87	-0.75	0.75	0.87	2.12	1.18
Fe/Au	-1.65	-2.11	-0.87	-0.29	0.29	0.87	2.11	1.65
Fe/Hg	-0.99	-1.84	-1.16	-0.93	0.93	1.16	1.84	0.99
FeN <sub>4</sub>	-1.38	-1.86	-0.94	-0.74	0.74	0.94	1.86	1.38

**Table S11.** The free energy change of every reaction step for ORR ( $\Delta G_a$ - $\Delta G_d$ ) and OER ( $\Delta G_e$ - $\Delta G_h$ ) on M/Fe.

	ORR				OER			
	$\Delta G_a$ (eV)	$\Delta G_b$ (eV)	$\Delta G_c$ (eV)	$\Delta G_d$ (eV)	$\Delta G_e$ (eV)	$\Delta G_f$ (eV)	$\Delta G_g$ (eV)	$\Delta G_h$ (eV)
Sc/Fe	0.17	-0.95	-4.56	0.42	-0.42	4.56	0.95	-0.17
Ti/Fe	-0.78	-3.53	-0.06	-0.55	0.55	0.06	3.53	0.78
V/Fe	-3.42	-0.96	0.04	-0.58	0.58	0.04	0.96	3.42
Cr/Fe	-1.33	-2.81	-0.50	-0.28	0.28	0.50	2.81	1.33
Mn/Fe	-2.88	-1.27	-0.62	-0.15	0.15	0.62	1.27	2.88
Fe/Fe	-0.89	-2.08	-0.92	-1.03	1.03	0.92	2.08	0.89
Co/Fe	-0.54	-1.25	-1.75	-1.38	1.38	1.75	1.25	0.54
Ni/Fe	0.02	-0.90	-2.00	-2.04	2.04	2.00	0.90	-0.02
Cu/Fe	-0.40	-0.91	-2.15	-1.46	1.46	2.15	0.91	0.40
Zn/Fe	0.12	-1.37	-2.60	-1.07	1.07	2.60	1.37	-0.12
Y/Fe	0.13	-0.01	-2.47	-2.57	2.57	2.47	0.01	-0.13
Zr/Fe	0.23	-4.30	1.23	-2.08	2.08	-1.23	4.30	-0.23
Nb/Fe	0.07	-4.57	1.46	-1.88	1.88	-1.46	4.57	-0.07
Mo/Fe	-0.02	-4.60	1.53	-1.83	1.83	-1.53	4.60	0.02
Tc/Fe	0.05	-3.74	0.56	-1.79	1.79	-0.56	3.74	-0.05
Ru/Fe	-0.74	-2.19	-0.91	-1.08	1.08	0.91	2.19	0.74
Rh/Fe	-0.93	-1.06	-2.01	-0.92	0.92	2.01	1.06	0.93
Pd/Fe	0.12	-0.49	-2.28	-2.27	2.27	2.28	0.49	-0.12
Ag/Fe	-0.09	0.41	-2.38	-2.86	2.86	2.38	-0.41	0.09
Cd/Fe	0.02	0.17	-2.27	-2.84	2.84	2.27	-0.17	-0.02
La/Fe	-0.05	0.12	-2.24	-2.75	2.75	2.24	-0.12	0.05
Hf/Fe	0.04	-4.47	1.34	-1.83	1.83	-1.34	4.47	-0.04
Ta/Fe	-0.19	-4.37	1.27	-1.63	1.63	-1.27	4.37	0.19
W/Fe	-0.18	-4.48	1.37	-1.63	1.63	-1.37	4.48	0.18
Re/Fe	-0.12	-4.11	0.98	-1.67	1.67	-0.98	4.11	0.12
Os/Fe	-0.51	-2.60	-0.56	-1.25	1.25	0.56	2.60	0.51
Ir/Fe	-0.53	-1.36	-1.76	-1.27	1.27	1.76	1.36	0.53
Pt/Fe	0.01	-0.73	-2.19	-2.01	2.01	2.19	0.73	-0.01
Au/Fe	-0.38	-0.33	-2.05	-2.16	2.16	2.05	0.33	0.38
Hg/Fe	-0.08	0.27	-2.27	-2.84	2.84	2.27	-0.27	0.08

**Table S12.** Calculated theoretical overpotentials for HER ( $\eta^{\text{HER}}$ ), ORR ( $\eta^{\text{ORR}}$ ) and OER ( $\eta^{\text{OER}}$ ) as well as their corresponding potential-determining step (PDS) on Fe/M.

Fe/M	$\eta^{\text{HER}}$ (V)	$\eta^{\text{ORR}}$ (V)	PDS for ORR	$\eta^{\text{OER}}$ (V)	PDS for OER
Fe/Sc	-0.48	0.49	$\text{OH}^* \rightarrow \text{H}_2\text{O}$	0.76	$\text{O}^* \rightarrow \text{OOH}^*$
Fe/Ti	-1.16	0.94	$\text{O}_2 \rightarrow \text{OOH}^*$	0.55	$\text{O}^* \rightarrow \text{OOH}^*$
Fe/V	-1.30	1.03	$\text{O}_2 \rightarrow \text{OOH}^*$	0.49	$\text{O}^* \rightarrow \text{OOH}^*$
Fe/Cr	-0.50	0.37	$\text{OH}^* \rightarrow \text{H}_2\text{O}$	0.81	$\text{O}^* \rightarrow \text{OOH}^*$
Fe/Mn	-0.74	0.49	$\text{O}^* \rightarrow \text{OH}^*$	0.93	$\text{O}^* \rightarrow \text{OOH}^*$
Fe/Fe	-0.73	0.34	$\text{O}_2 \rightarrow \text{OOH}^*$	0.85	$\text{O}^* \rightarrow \text{OOH}^*$
Fe/Co	-0.59	0.31	$\text{O}^* \rightarrow \text{OH}^*$	0.84	$\text{O}^* \rightarrow \text{OOH}^*$
Fe/Ni	-0.41	0.54	$\text{OH}^* \rightarrow \text{H}_2\text{O}$	0.88	$\text{O}^* \rightarrow \text{OOH}^*$
Fe/Cu	-0.02	0.90	$\text{OH}^* \rightarrow \text{H}_2\text{O}$	0.89	$\text{O}^* \rightarrow \text{OOH}^*$
Fe/Zn	-0.67	0.36	$\text{O}^* \rightarrow \text{OH}^*$	0.87	$\text{O}^* \rightarrow \text{OOH}^*$
Fe/Y	-0.53	0.49	$\text{OH}^* \rightarrow \text{H}_2\text{O}$	0.65	$\text{O}^* \rightarrow \text{OOH}^*$
Fe/Zr	-0.83	0.58	$\text{O}^* \rightarrow \text{OH}^*$	1.15	$\text{O}^* \rightarrow \text{OOH}^*$
Fe/Nb	-1.41	1.02	$\text{O}_2 \rightarrow \text{OOH}^*$	0.43	$\text{H}_2\text{O} \rightarrow \text{OH}^*$
Fe/Mo	-1.48	1.05	$\text{O}_2 \rightarrow \text{OOH}^*$	0.60	$\text{OH}^* \rightarrow \text{O}^*$
Fe/Tc	-1.46	1.05	$\text{O}_2 \rightarrow \text{OOH}^*$	0.41	$\text{H}_2\text{O} \rightarrow \text{OH}^*$
Fe/Ru	-0.88	0.59	$\text{O}_2 \rightarrow \text{OOH}^*$	0.72	$\text{O}^* \rightarrow \text{OOH}^*$
Fe/Rh	-0.18	0.63	$\text{OH}^* \rightarrow \text{H}_2\text{O}$	0.46	$\text{O}^* \rightarrow \text{OOH}^*$
Fe/Pd	-0.43	0.49	$\text{OH}^* \rightarrow \text{H}_2\text{O}$	0.89	$\text{O}^* \rightarrow \text{OOH}^*$
Fe/Ag	-0.35	0.61	$\text{OH}^* \rightarrow \text{H}_2\text{O}$	0.83	$\text{O}^* \rightarrow \text{OOH}^*$
Fe/Cd	-0.76	0.35	$\text{O}_2 \rightarrow \text{OOH}^*$	0.70	$\text{O}^* \rightarrow \text{OOH}^*$
Fe/La	-0.40	0.57	$\text{OH}^* \rightarrow \text{H}_2\text{O}$	0.86	$\text{O}^* \rightarrow \text{OOH}^*$
Fe/Hf	-0.91	0.38	$\text{OH}^* \rightarrow \text{H}_2\text{O}$	0.27	$\text{O}^* \rightarrow \text{OOH}^*$
Fe/Ta	-1.48	1.07	$\text{O}_2 \rightarrow \text{OOH}^*$	0.48	$\text{H}_2\text{O} \rightarrow \text{OH}^*$
Fe/W	-1.59	1.09	$\text{O}_2 \rightarrow \text{OOH}^*$	0.65	$\text{OH}^* \rightarrow \text{O}^*$
Fe/Re	-1.52	1.05	$\text{O}_2 \rightarrow \text{OOH}^*$	0.67	$\text{OH}^* \rightarrow \text{O}^*$
Fe/Os	-1.06	0.79	$\text{O}_2 \rightarrow \text{OOH}^*$	0.57	$\text{O}^* \rightarrow \text{OOH}^*$
Fe/Ir	-0.60	0.34	$\text{O}_2 \rightarrow \text{OOH}^*$	0.74	$\text{O}^* \rightarrow \text{OOH}^*$
Fe/Pt	-0.45	0.48	$\text{OH}^* \rightarrow \text{H}_2\text{O}$	0.89	$\text{O}^* \rightarrow \text{OOH}^*$
Fe/Au	-0.05	0.94	$\text{OH}^* \rightarrow \text{H}_2\text{O}$	0.88	$\text{O}^* \rightarrow \text{OOH}^*$
Fe/Hg	-0.75	0.30	$\text{OH}^* \rightarrow \text{H}_2\text{O}$	0.61	$\text{O}^* \rightarrow \text{OOH}^*$
FeN <sub>4</sub>	-0.25	0.49	$\text{OH}^* \rightarrow \text{H}_2\text{O}$	0.63	$\text{O}^* \rightarrow \text{OOH}^*$

**Table S13.** Calculated theoretical overpotentials for HER ( $\eta^{\text{HER}}$ ), ORR ( $\eta^{\text{ORR}}$ ) and OER ( $\eta^{\text{OER}}$ ) as well as their corresponding potential-determining step (PDS) on M/Fe.

Fe/M	$\eta^{\text{HER}}$ (V)	$\eta^{\text{ORR}}$ (V)	PDS for ORR	$\eta^{\text{OER}}$ (V)	PDS for OER
Sc/Fe	-2.03	1.65	$\text{O}_2 \rightarrow \text{OOH}^*$	3.33	$\text{H}_2\text{O} \rightarrow \text{OH}^*$
Ti/Fe	-1.93	1.17	$\text{O}^* \rightarrow \text{OH}^*$	2.30	$\text{O}^* \rightarrow \text{OOH}^*$
V/Fe	-1.75	1.27	$\text{O}^* \rightarrow \text{OH}^*$	2.19	$\text{O}^* \rightarrow \text{OOH}^*$
Cr/Fe	-0.61	0.95	$\text{OH}^* \rightarrow \text{H}_2\text{O}$	1.58	$\text{OOH}^* \rightarrow \text{O}_2$
Mn/Fe	-0.04	1.08	$\text{OH}^* \rightarrow \text{H}_2\text{O}$	1.65	$\text{OOH}^* \rightarrow \text{O}_2$
Fe/Fe	-0.73	0.34	$\text{O}_2 \rightarrow \text{OOH}^*$	0.85	$\text{H}_2\text{O} \rightarrow \text{OH}^*$
Co/Fe	-0.59	0.69	$\text{O}_2 \rightarrow \text{OOH}^*$	0.52	$\text{H}_2\text{O} \rightarrow \text{OH}^*$
Ni/Fe	-1.57	1.25	$\text{O}_2 \rightarrow \text{OOH}^*$	0.81	$\text{H}_2\text{O} \rightarrow \text{OH}^*$
Cu/Fe	-1.23	0.83	$\text{O}_2 \rightarrow \text{OOH}^*$	0.92	$\text{H}_2\text{O} \rightarrow \text{OH}^*$
Zn/Fe	-2.62	1.35	$\text{O}_2 \rightarrow \text{OOH}^*$	1.37	$\text{H}_2\text{O} \rightarrow \text{OH}^*$
Y/Fe	-2.49	1.36	$\text{O}_2 \rightarrow \text{OOH}^*$	1.34	$\text{H}_2\text{O} \rightarrow \text{OH}^*$
Zr/Fe	-2.17	2.46	$\text{O}^* \rightarrow \text{OH}^*$	3.07	$\text{O}^* \rightarrow \text{OOH}^*$
Nb/Fe	-1.99	2.69	$\text{O}^* \rightarrow \text{OH}^*$	3.34	$\text{O}^* \rightarrow \text{OOH}^*$
Mo/Fe	-1.78	2.76	$\text{O}^* \rightarrow \text{OH}^*$	3.37	$\text{O}^* \rightarrow \text{OOH}^*$
Tc/Fe	-1.58	1.79	$\text{O}^* \rightarrow \text{OH}^*$	2.51	$\text{O}^* \rightarrow \text{OOH}^*$
Ru/Fe	-0.51	0.49	$\text{O}_2 \rightarrow \text{OOH}^*$	0.96	$\text{H}_2\text{O} \rightarrow \text{OH}^*$
Rh/Fe	-0.31	0.31	$\text{OH}^* \rightarrow \text{H}_2\text{O}$	0.78	$\text{OOH}^* \rightarrow \text{O}_2$
Pd/Fe	-1.95	1.35	$\text{O}_2 \rightarrow \text{OOH}^*$	1.05	$\text{H}_2\text{O} \rightarrow \text{OH}^*$
Ag/Fe	-0.78	1.64	$\text{OH}^* \rightarrow \text{H}_2\text{O}$	4.63	$\text{OH}^* \rightarrow \text{O}^*$
Cd/Fe	-0.19	1.40	$\text{OOH}^* \rightarrow \text{O}^*$	1.61	$\text{OH}^* \rightarrow \text{O}^*$
La/Fe	-0.31	1.35	$\text{OOH}^* \rightarrow \text{O}^*$	1.52	$\text{OH}^* \rightarrow \text{O}^*$
Hf/Fe	-2.05	2.57	$\text{O}^* \rightarrow \text{OH}^*$	3.24	$\text{O}^* \rightarrow \text{OOH}^*$
Ta/Fe	-1.82	2.50	$\text{O}^* \rightarrow \text{OH}^*$	3.14	$\text{O}^* \rightarrow \text{OOH}^*$
W/Fe	-1.67	2.60	$\text{O}^* \rightarrow \text{OH}^*$	3.25	$\text{O}^* \rightarrow \text{OOH}^*$
Re/Fe	-1.50	2.21	$\text{O}^* \rightarrow \text{OH}^*$	2.88	$\text{O}^* \rightarrow \text{OOH}^*$
Os/Fe	-0.76	0.67	$\text{O}_2 \rightarrow \text{OOH}^*$	1.37	$\text{H}_2\text{O} \rightarrow \text{OH}^*$
Ir/Fe	-0.25	0.70	$\text{O}_2 \rightarrow \text{OOH}^*$	0.53	$\text{H}_2\text{O} \rightarrow \text{OH}^*$
Pt/Fe	-1.45	1.24	$\text{O}_2 \rightarrow \text{OOH}^*$	0.96	$\text{H}_2\text{O} \rightarrow \text{OH}^*$
Au/Fe	-1.75	0.85	$\text{OOH}^* \rightarrow \text{O}^*$	0.93	$\text{OH}^* \rightarrow \text{O}^*$
Hg/Fe	-0.77	1.50	$\text{OOH}^* \rightarrow \text{O}^*$	1.61	$\text{OH}^* \rightarrow \text{O}^*$

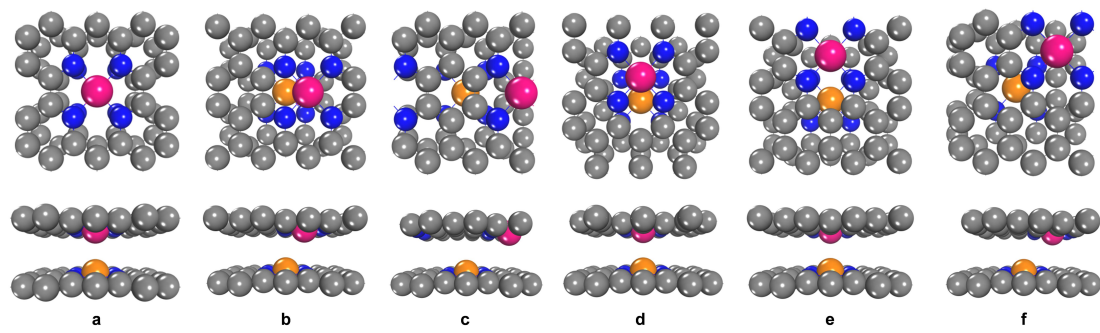


**Fig. S2.** Top and side views of initial trial configurations for B-SACs. The gray, blue, orange, and magenta spheres indicate the C, N, Fe, and transition metal atoms, respectively.

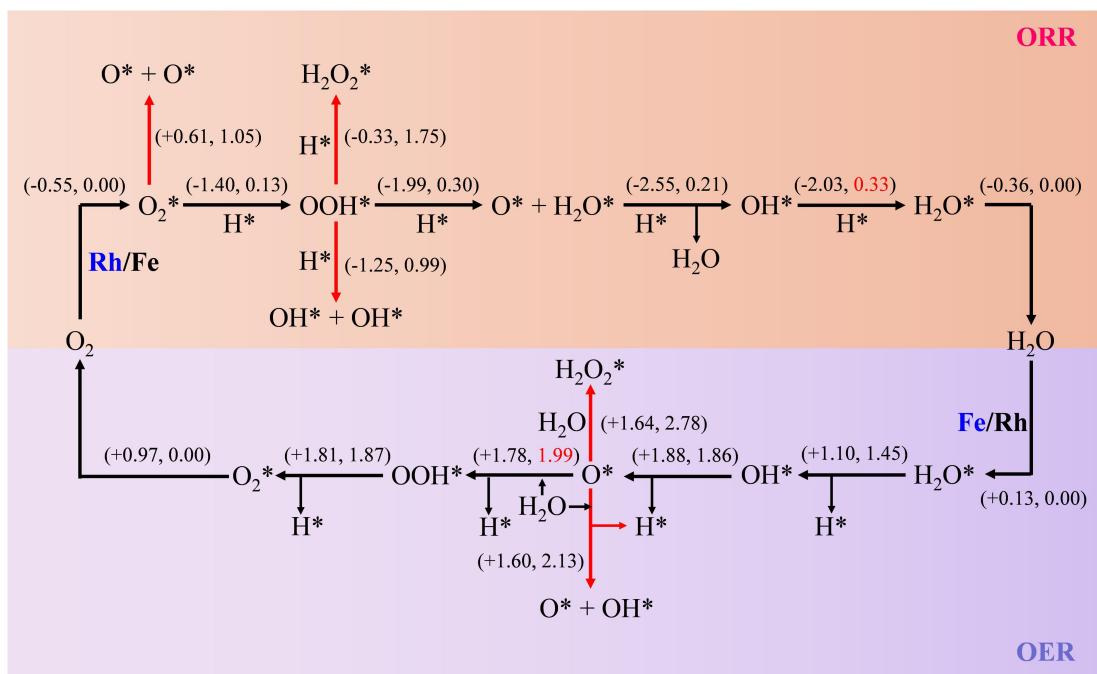


**Fig. S3.** The possible reaction pathways for ORR and OER on Rh/Fe and Fe/Rh. The number in the parentheses are the reaction heat (the former) and the energy barrier (the later) in unit of eV.

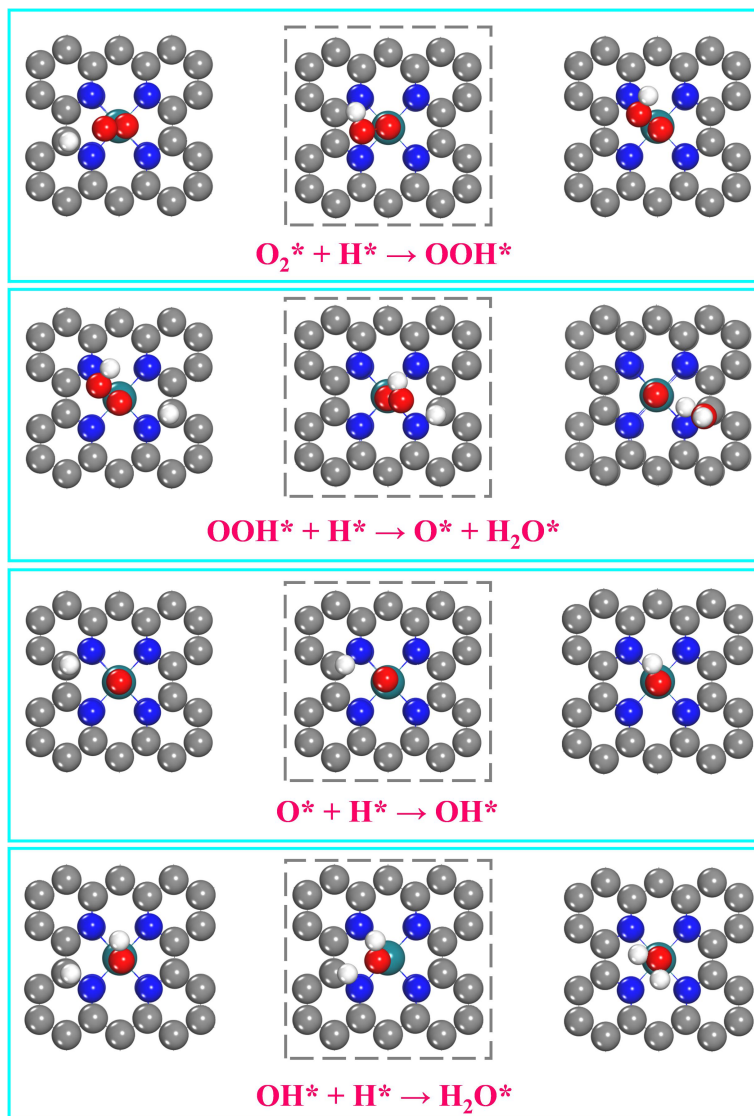


**Fig. S4.** Atomic structures of the initial states, transition states (middle panel), and final states of the minimum energy pathway for ORR on Rh/Fe.

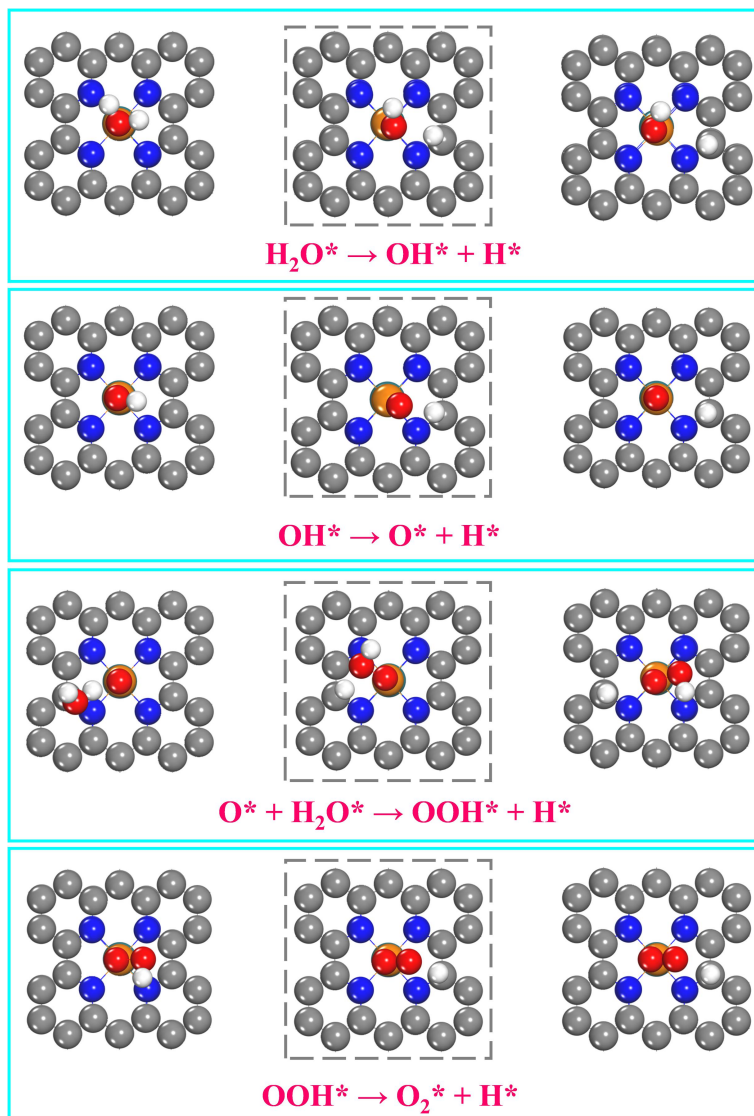


**Fig. S5.** Atomic structures of the initial states, transition states (middle panel), and final states of the minimum energy pathway for OER on Fe/Rh.

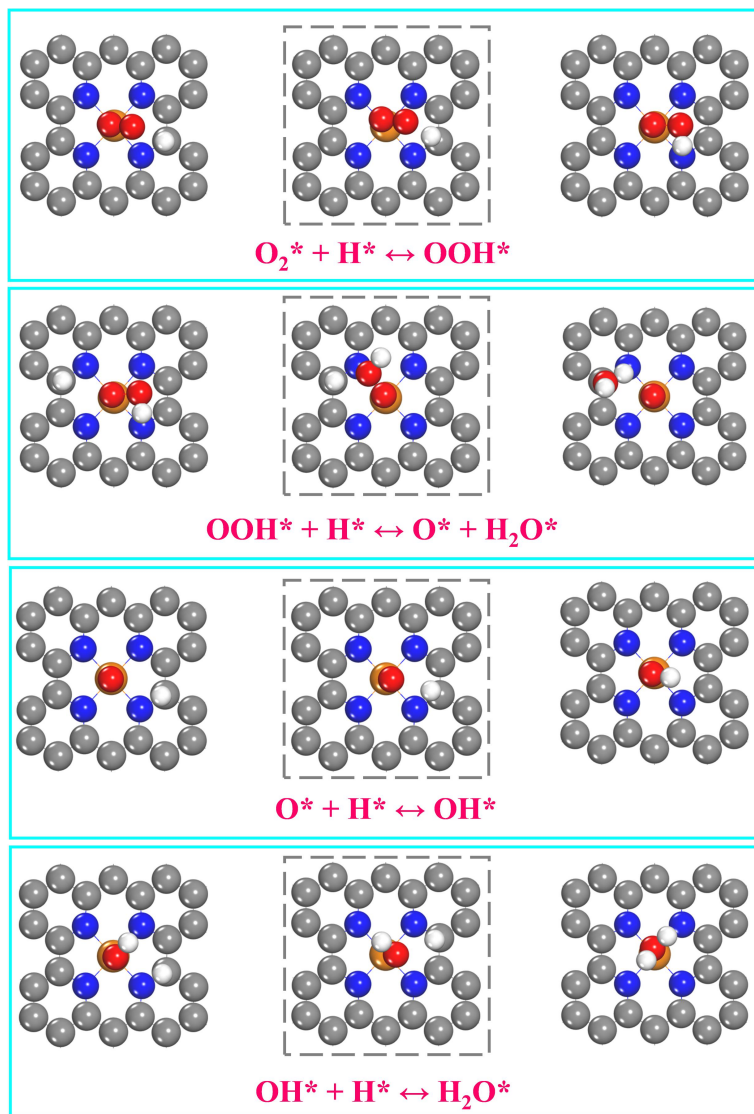


**Fig. S6.** Atomic structures of the initial states, transition states (middle panel), and final states of the minimum energy pathway for ORR (from left to right) and OER (from right to left) on Fe/Hf.

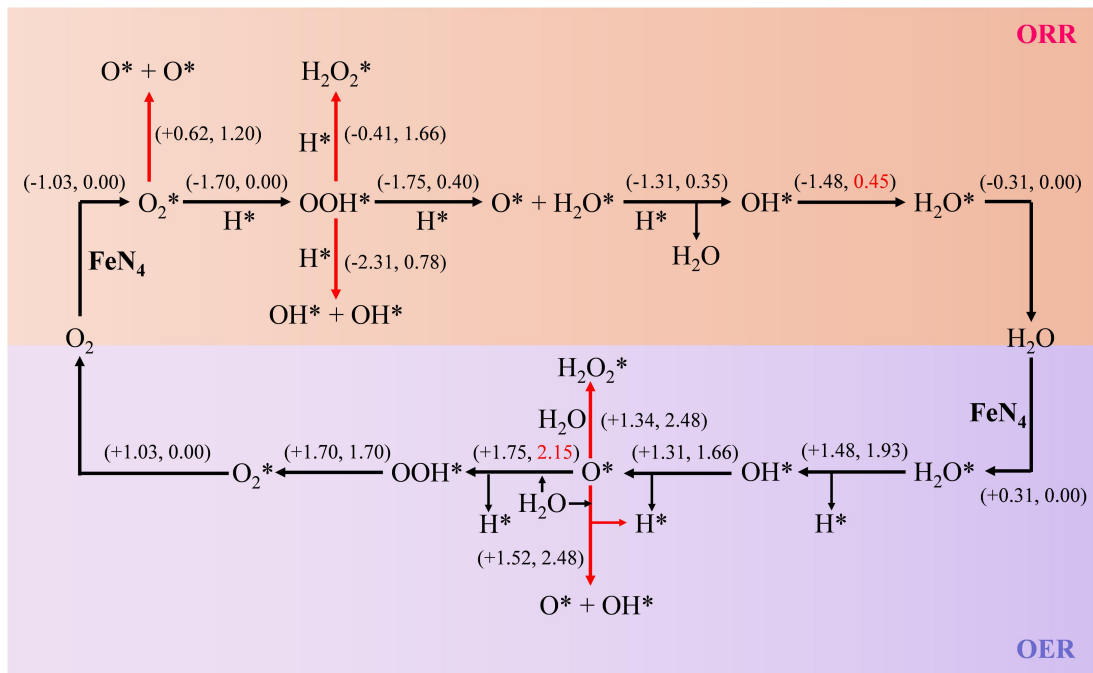


**Fig. S7.** The possible reaction pathways for ORR and OER on monolayer  $FeN_4$ . The number in the parentheses are the reaction heat (the former) and the energy barrier (the later) in unit of eV.

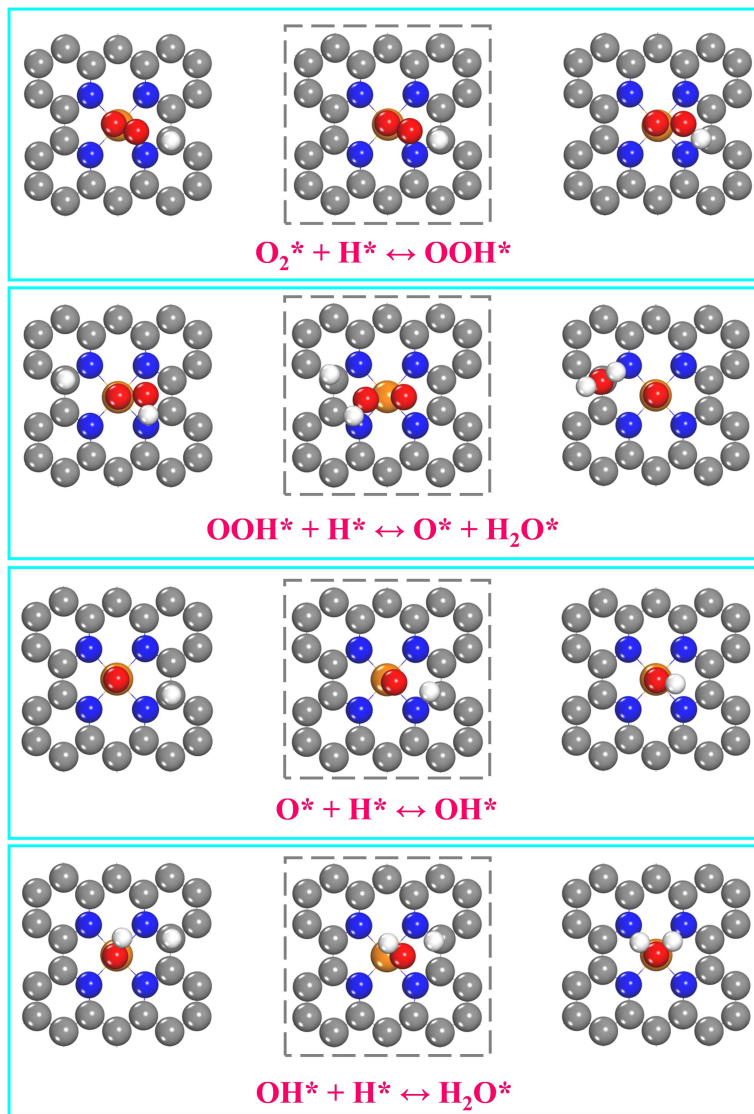


**Fig. S8.** Atomic structures of the initial states, transition states (middle panel), and final states of the minimum energy pathway for ORR (from left to right) and OER (from right to left) on monolayer  $FeN_4$ .

## References

- [1] S. Kattel, P. Atanassov and B. Kiefer, *J. Phys. Chem. C*, 2012, **116**, 8161-8166.
- [2] X. Cao, X.-F. Li and W. Hu, *Chem.-Asian J.*, 2018, **13**, 3239-3245.
- [3] S. Kattel and G. Wang, *J. Mater. Chem. A*, 2013, **1**, 10790-10797.
- [4] H. Xu, D. Cheng, D. Cao and X. C. Zeng, *Nat. Catal.*, 2018, **1**, 339-348.
- [5] Z. Zhang, J. Xiao, X.-J. Chen, S. Yu, L. Yu, R. Si, Y. Wang, S. Wang, X. Meng, Y. Wang, Z.-Q. Tian and D. Deng, *Angew. Chem. Int. Edit.*, 2018, **57**, 16339-16342.
- [6] Y. Wang, Y.-J. Tang and K. Zhou, *J. Am. Chem. Soc.*, 2019, **141**, 14115-14119.